Engineering Letters

Dual Wind Effects on Predator-Prey Dynamics: Global Stability and Persistence in a Modified Leslie-Gower Model with Adaptive Harvesting

Fengde Chen, Lanqi Luo, Yuting Huang, and Guangwen He

Abstract—**This paper addresses the limitations of traditional predator-prey models by constructing a modified Leslie-Gower model that incorporates the dual effects of wind on predator foraging efficiency and human harvesting activities. We introduce nonlinear functions $\phi_1(\omega) = 1 + k_1\omega$ and $\phi_2(\omega) = 1 + k_2\omega$ to quantify the dynamic impacts of wind speed on predator search efficiency (negatively correlated) and human harvesting intensity (negatively correlated). Through differential equation theory, we analyze the local/global stability of boundary and positive equilibria, system persistence, and parameter sensitivity, supported by numerical simulations. Key findings include: (1) Wind speeds exceeding a critical threshold enable prey populations to overcome extinction thresholds, ensuring persistent survival. (2) Human harvesting efficiency significantly decreases with increasing wind speed. (3) Predator density exhibits non-monotonic variation with wind speed, while prey density monotonically increases, asymptotically approaching environmental carrying capacity. (4) The existence of a positive equilibrium guarantees global asymptotic stability, highlighting the crucial role of wind effects in maintaining system equilibrium. This study provides theoretical foundations for ecosystem management under extreme climates and supports wind-direction strategies in fishery conservation.**

Index Terms—**Leslie-Gower model, predator-prey system, wind effects, stability analysis, persistence**

I. INTRODUCTION

IN nature, the predator-prey relationship is one of the most fundamental interspecific relationships. As a result, research on predator-prey relationships has been a long-standing focus for biomathematicians, as seen in [1]-[11] and the references therein. Previous studies have primarily concentrated on interspecific relationships, exploring the impact of various functional response functions on the dynamic behavior of systems, with few scholars investigating the influence of environmental variables on ecosystems. It is well known that wind plays a significant role in predator-prey relationships. For instance, wind exposure at nest sites can enhance the visibility of nests to aerial predators, thereby potentially elevating the predation risk for the species [16]. Building upon this ecological premise, Jawad, Sultan, and Winter [17] introduced a predator-prey model that incorporates the influence of wind effects.

$$\begin{aligned} \frac{du}{dt} &= ru\Big(1-\frac{u}{K}\Big)-\frac{\alpha uv}{\phi(\omega)}-equ, \\ \frac{dv}{dt} &= sv\Big(1-\frac{v}{\phi(\omega)+\beta u+c}\Big)-\gamma v. \end{aligned} \tag{1}$$

The authors thoroughly examined the dynamic behavior of this model. However, the numerical simulations in [17] showed that as wind speed increases, the population densities of both predators and prey increase, which does not align with the aforementioned ecological background. Recently, Huang, Chen, Zhu, and Li [18] argued that model (1) does not reflect reality and proposed a more reasonable model:

$$\begin{aligned} \frac{du}{dt} &= ru\Big(1-\frac{u}{K}\Big)-\alpha\phi(\omega)uv-equ, \\ \frac{dv}{dt} &= sv\Big(1-\frac{v}{\beta\phi(\omega)u+c}\Big). \end{aligned} \tag{2}$$

The authors gave a thoroughly investigation about the dynamic behaviors of the system (2). However, when considering more practical scenarios, model (2) still has some shortcomings.

Firstly, model (2) uses $\alpha\phi(\omega)uv$ to describe the predation efficiency of predators on prey, where the predation efficiency is a monotonically increasing function of wind. In reality, the impact of wind on predator behavior is generally negative [19]. Wind can alter the prey's perception and activity patterns. For instance, strong winds may mask the scent or sound of prey, reducing the detection efficiency of predators. Wind can also affect the escape behavior of prey. For example, small mammals or insects may reduce their activity in strong winds to lower the risk of predation[19][20][21]. Wind may also affect the search efficiency of predators. For instance, avian predators may find it more difficult to locate prey in strong winds [22]. Additionally, wind can change the predation strategies of predators. Some predators may choose to be active during periods of weaker wind [22]. Therefore, in a predator-prey system, it is more appropriate for the functional response function of predators to be a monotonically decreasing function of wind. This indicates the necessity of proposing a more suitable predator-prey model that reflects the decrease in predation efficiency with increasing wind speed.

Secondly, model (2) uses equ to represent human harvesting, assuming that human harvesting is independent of wind. In reality, human harvesting is significantly affected by wind. For example, in African hunting studies, wind direction and

---

Manuscript received Feb 16, 2025, revised May 23, 2025. This work is supported by the Natural Science Foundation of Fujian Province(2024J01273).

F. D. Chen is a professor of College of Mathematics and Statistics, Fuzhou University, Fuzhou, CHINA (e-mail: fdchen@fzu.edu.cn).

L. Q. Luo is a postgraduate student of College of Mathematics and Statistics, Fuzhou University, Fuzhou, CHINA (e-mail: 2059667486@qq.com).

Y. T. Huang is a postgraduate student of College of Mathematics and Statistics, Fuzhou University, Fuzhou, CHINA (e-mail: 1104943637@qq.com).

G. W. He is a postgraduate student of College of Mathematics and Statistics, Fuzhou University, Fuzhou, CHINA (e-mail: 594047408@qq.com).

speed have been found to significantly influence the success rate of hunters. Hunters typically choose upwind positions to avoid prey detecting human scent. Strong winds can also mask the sound of prey, increasing tracking difficulty[23]. In fishing activities in the North American Great Lakes, wind direction and speed have been found to affect fish distribution and fishing success rates. For instance, strong winds can increase wave height, causing fish to move to deeper waters, thereby altering fishing strategies [24]. In entomological studies, wind direction and speed can affect the efficiency of insect trapping. For example, when trapping moths or butterflies, strong winds can make it difficult for insects to fly or alter their flight paths, affecting trapping outcomes[25]. In bird studies, wind direction and speed can influence bird migration paths and flight altitudes, thereby affecting the efficiency of bird trapping. For example, tailwind conditions can increase bird flight speed, making trapping more difficult[26]. In traditional fishing activities on Pacific islands, wind direction and speed are considered key factors determining fishing success. Fishermen choose fishing locations and times based on wind direction [27]. This indicates that the harvesting term must account for the influence of wind.

Based on the above analysis, we propose the following model that better aligns with the actual ecological background:

$$\begin{aligned} \frac{du}{dt} &= ru\Big(1-\frac{u}{K}\Big)-\frac{\alpha uv}{\phi_1(\omega)}-\frac{equ}{\phi_2(\omega)}, \\ \frac{dv}{dt} &= sv\left(1-\frac{v}{\dfrac{\beta u}{\phi_1(\omega)}+c}\right), \end{aligned} \tag{3}$$

where the variables u and v represent the population densities of prey and predator species at a given time, respectively. $r, K, \alpha, e, q, s, \beta, c$ are positive constants.

We make the following assumptions to model the system dynamics:

1. Prey population dynamics The prey population is characterized by its intrinsic growth rate, environmental carrying capacity K, predation rate α, and human harvesting, which is quantified by the harvesting effort c and harvesting coefficient q.

2. Predator population dynamics The predator population is governed by its intrinsic growth rate s and environmental carrying capacity $\frac{\beta u}{\phi_1(\omega)}+c$, where c represents supplementary food sources available to the predator species.

3. Predator-prey interaction and wind effects The predator-prey interaction is modeled using a Lotka-Volterra type functional response αu, where the number of prey captured by predators is given by $\frac{\alpha uv}{\phi_1(\omega)}$. The wind efficiency function $\phi_1(\omega)=1+k_1\omega$ incorporates wind speed ω through a positive constant k_1, under the following assumptions:

(a) Under windless conditions ($\omega = 0$), the predator's search efficiency remains at its baseline level, i.e., $\phi_1(0)=1$;

(b) The predator's search efficiency decreases monotonically with increasing wind speed, while remaining positive for all ω, i.e., $\phi_1(\omega)>0$.

4. Wind effects on human harvesting The impact of wind on human harvesting is modeled by the term $\frac{equ}{\phi_2(\omega)}$, where the wind efficiency function $\phi_2(\omega)=1+k_2\omega$ incorporates wind speed ω through a positive proportionality constant k_2. This formulation is based on two key assumptions:

(a) Under windless conditions ($\omega = 0$), the harvesting rate remains at its baseline level, i.e., $\phi_2(0)=1$;

(b) The harvesting efficiency exhibits an inverse relationship with wind speed, maintaining positivity throughout the operational range, i.e., $\phi_2(\omega)>0$.

This paper aims to comprehensively analyze the dynamic behavior of system (3) and elucidate the role of wind effects in shaping the system's dynamics. The structure of the paper is organized as follows: Section 2 establishes the fundamental properties of the solutions, including their positivity and boundedness; Section 3 investigates the existence and local stability of equilibrium points; Section 4 investigates the extinction property of the system; Section 5 extends the analysis of local stability to global stability; Section 6 explores the conditions for system persistence; Section 7 investigates the effect of wind; Section 8 investigates the dynamical behaviors under extreme scenarios; Section 9 validates the theoretical results through numerical simulations; and finally, the concluding section synthesizes the influence of wind effects on the system's dynamics and underscores the novel contributions of this study.

II. POSITIVITY AND BOUNDEDNESS OF SOLUTIONS TO SYSTEM (3)

Regarding the positivity of solutions to system (3), we have the following result.

Theorem 2.1 *The non-negative quadrant $R_2^+ = \{(u,v)\in R^2 \mid u>0, v>0\}$ is positively invariant under the dynamics of system (3).*

Proof From (3), for all $t\in[0,+\infty)$, we have:

$$\begin{aligned} u(t) &= u(0)\exp\left\{\int_0^t \Gamma_1 dt\right\}>0, \\ v(t) &= v(0)\exp\left\{\int_0^t \Gamma_2 dt\right\}>0 \end{aligned}$$

where

$$\begin{aligned} \Gamma_1 &= r\Big(1-\frac{u}{K}\Big)-\frac{\alpha v}{\phi_1(\omega)}-\frac{eq}{\phi_2(\omega)}, \\ \Gamma_2 &= s\left(1-\frac{v}{\dfrac{\beta u}{\phi_1(\omega)}+c}\right). \end{aligned} \tag{4}$$

Thus, Theorem 2.1 is proven.

Theorem 2.2 *The solutions $u(t)$ and $v(t)$ of system (3) with initial conditions $u(0)>0$ and $v(0)>0$ are uniformly bounded.*

Proof

From the first equation of system (3), we derive the inequality:

$$\frac{du}{dt}\le ru\left(1-\frac{u}{K}\right),$$

which describes the upper bound of the prey population growth. Applying Lemma 2.3 from [35] to this inequality, we establish the following result:

$$\limsup_{t\to+\infty} u(t) \le K. \tag{5}$$

This implies that the prey population $u(t)$ is asymptotically bounded above by the carrying capacity K. Consequently, for any sufficiently small positive constant $\varepsilon > 0$, there exists a time $T_1 > 0$ such that for all $t \ge T_1$, the following inequality holds:

$$u(t) < K + \varepsilon. \tag{6}$$

For $t \ge T_1$, combining the second equation of system (3) with inequality (6), we derive the following upper bound for the predator population growth:

$$\begin{aligned}\frac{dv}{dt} &= sv\left(1 - \frac{v}{\frac{\beta u}{\phi_1(\omega)} + c}\right)\\ &\le sv\left(1 - \frac{v}{\frac{\beta(K+\varepsilon)}{\phi_1(\omega)} + c}\right).\end{aligned}$$

Applying Lemma 2.3 from [35] to this inequality, we obtain the asymptotic bound for the predator population:

$$\limsup_{t\to+\infty} v(t) \le \frac{\beta(K+\varepsilon)}{\phi_1(\omega)} + c. \tag{7}$$

Since ε is an arbitrarily small positive constant, taking the limit as $\varepsilon \to 0$ in (7) yields:

$$\limsup_{t\to+\infty} v(t) \le \frac{\beta K}{\phi_1(\omega)} + c. \tag{8}$$

The inequalities (5) and (8) demonstrate that the solutions $u(t)$ and $v(t)$ of system (3), with initial conditions $u(0) > 0$ and $v(0) > 0$, are uniformly bounded. This completes the proof of Theorem 2.2.

III. EXISTENCE AND LOCAL STABILITY OF EQUILIBRIUM POINTS IN SYSTEM (3)

Regarding the existence of equilibrium points in system (3), we have the following result.

Theorem 3.1 *System (3) always admits two boundary equilibrium points: the vanishing equilibrium $E_0(0,0)$, where both prey and predator populations are extinct, and the prey-free equilibrium $E_2(0,c)$, where the prey population is extinct while the predator population stabilizes at c. Furthermore, under the condition $\phi_2(\omega)r > qe$, there exists a predator-free equilibrium $E_1(\pi,0)$, where the prey population stabilizes at $\pi = \frac{K(\phi_2(\omega)r-qe)}{\phi_2(\omega)r}$ and the predator population is extinct.*

Additionally, if the following condition holds:

$$\phi_2(\omega)\, r\phi_1(\omega) > \phi_2(\omega)\,\alpha c + eq\phi_1(\omega), \tag{9}$$

then there exists a unique positive equilibrium point $E_2(u^*, v^*)$, where:

$$u^* = -\frac{\Delta(\omega)}{\phi_2(\omega)\left(K\alpha\beta + r\phi_1(\omega)^2\right)}, \tag{10}$$

and v^* satisfies $v^* = \frac{\beta u^*}{\phi_1(\omega)} + c$, where

$$\begin{aligned}\Delta(\omega) &= \phi_1(\omega)\, K\Big(\phi_2(\omega)\alpha c\\ &\qquad -\phi_2(\omega)\, r\phi_1(\omega) + eq\phi_1(\omega)\Big).\end{aligned} \tag{11}$$

Proof

The equilibrium points of system (3) satisfy the following equations:

$$\begin{aligned}&ru(1-\tfrac{u}{K}) - \frac{\alpha uv}{\phi_1(\omega)} - \frac{equ}{\phi_2(\omega)} = 0,\\ &sv\left(1 - \frac{v}{\dfrac{\beta u}{\phi_1(\omega)} + c}\right) = 0.\end{aligned} \tag{12}$$

From the second equation of (12), we obtain $v = 0$ or $v = \frac{\beta u}{\phi_1(\omega)} + c$. Substituting $v = 0$ into the first equation of (12), we obtain:

$$ru(1-\frac{u}{K}) - \frac{equ}{\phi_2(\omega)} = 0. \tag{13}$$

The solutions to equation (12) are $u_1 = 0$ and $u_2 = \frac{K(\phi_2(\omega)r-qe)}{\phi_2(\omega)r}$. Therefore, system (3) has a zero equilibrium point $E_0(0,0)$. Additionally, if the condition $\phi_2(\omega)r > qe$ holds, then there exists a predator-free equilibrium point $E_1(\pi,0)$.

Substituting $v = \frac{\beta u}{\phi_1(\omega)} + c$ into the first equation of (12), we obtain:

$$ru(1-\frac{u}{K}) - \frac{\alpha u(\dfrac{\beta u}{\phi_1(\omega)} + c)}{\phi_1(\omega)} - \frac{equ}{\phi_2(\omega)} = 0. \tag{14}$$

Under the condition (9), equation (14) has a unique positive solution u^*, where u^* is given by (10). Therefore, system (3) has a unique positive equilibrium point $E_2(u^*, v^*)$. This completes the proof of Theorem 3.1.

Theorem 3.2

The vanishing equilibrium $E_0(0,0)$ is always unstable. For the prey-free equilibrium $E_2(0,c)$, if the condition

$$\phi_2(\omega)r\phi_1(\omega) < \phi_2(\omega)\alpha c + eq\phi_1(\omega) \tag{15}$$

holds, then $E_2(0,c)$ is locally asymptotically stable. In contrast, the predator-free equilibrium $E_1(\pi,0)$ is always unstable. Furthermore, if the condition

$$\phi_2(\omega)r\phi_1(\omega) > \phi_2(\omega)\alpha c + eq\phi_1(\omega) \tag{16}$$

is satisfied, then the positive equilibrium $E_3(u^*, v^*)$ is locally asymptotically stable.

Proof The Jacobian matrix of system (3) is calculated as:

$$J = \begin{pmatrix} J_{11} & J_{12}\\ J_{21} & J_{22}\end{pmatrix} \tag{17}$$

where:

$$\begin{aligned}
J_{11} &= r\left(1-\frac{u}{K}\right)-\frac{ru}{K}-\frac{v\alpha}{\phi_1(\omega)}-\frac{eq}{\phi_2(\omega)},\\
J_{12} &= -\frac{\alpha u}{\phi_1(\omega)},\\
J_{21} &= \frac{s\,v^2\beta}{\left(\frac{\beta u}{\phi_1(\omega)}+c\right)^2\phi_1(\omega)},\\
J_{22} &= s\left(1-\frac{v}{\frac{\beta u}{\phi_1(\omega)}+c}\right)-\frac{sv}{\frac{\beta u}{\phi_1(\omega)}+c}.
\end{aligned}$$

The Jacobian matrix of system (3) evaluated at the vanishing equilibrium point $E_0(0,0)$ is given by:

$$J(E_0(0,0))=\begin{pmatrix}\dfrac{\phi_2(\omega)r-qe}{\phi_2(\omega)} & 0\\ 0 & s\end{pmatrix}.$$

The eigenvalues of $J(E_0)$ are $\lambda_1=\frac{\phi_2(\omega)r-qe}{\phi_2(\omega)}$ and $\lambda_2=s>0$. Therefore, $E_0(0,0)$ is unstable.

The Jacobian matrix of system (3) at the predator-free equilibrium point $E_1(\overline{u},0)$ is:

$$J(E_1(\overline{u},0))=\begin{pmatrix}A_{11} & A_{12}\\ 0 & s\end{pmatrix},$$

where:

$$\begin{aligned}
A_{11} &= r\left(1-\frac{\phi_2(\omega)r-qe}{\phi_2(\omega)r}\right)-\frac{\phi_2(\omega)r-qe}{\phi_2(\omega)}-\frac{qe}{\phi_2(\omega)}\\
&= -\frac{\phi_2(\omega)r-qe}{\phi_2(\omega)},\\
A_{12} &= -\frac{\alpha K(\phi_2(\omega)r-qe)}{\phi_2(\omega)r\phi_1(\omega)}.
\end{aligned}$$

The eigenvalues of $J(E_1)$ are $\lambda_1=A_{11}$ and $\lambda_2=s>0$. Therefore, $E_1(\overline{u},0)$ is unstable.

The Jacobian matrix of system (3) at the prey-free equilibrium point $E_2(0,c)$ is:

$$J(E_2(0,c))=\begin{pmatrix}B_{11} & 0\\ \frac{s\beta}{\phi_1(\omega)} & -s\end{pmatrix},$$

where:

$$\begin{aligned}
B_{11} &= r-\frac{c\alpha}{\phi_1(\omega)}-\frac{qe}{\phi_2(\omega)}\\
&= \frac{-\phi_2(\omega)\alpha c+\phi_2(\omega)r\phi_1(\omega)-eq\phi_2(\omega)}{\phi_1(\omega)\phi_2(\omega)}.
\end{aligned}$$

The eigenvalues of $J(E_2)$ are $\lambda_1=B_{11}$ and $\lambda_2=-s<0$. Therefore, when condition (15) holds, $E_2(0,c)$ is locally asymptotically stable.

The positive equilibrium point $E_3(u^*,v^*)$ of system (3) is determined by the following system of equations:

$$\begin{aligned}
r(1-\tfrac{u^*}{K})-\frac{\alpha v^*}{\phi_1(\omega)}-\frac{eq}{\phi_2(\omega)}=0,\\
s\left(1-\frac{v^*}{\dfrac{\beta u^*}{\phi_1(\omega)}+c}\right)=0.
\end{aligned}\tag{18}$$

The Jacobian matrix of system (3) at the positive equilibrium point $E_3(u^*,v^*)$ is:

$$J(E_3(u^*,v^*))=\begin{pmatrix}D_{11} & D_{12}\\ D_{21} & D_{22}\end{pmatrix},$$

where:

$$\begin{aligned}
D_{11} &= r\left(1-\frac{u^*}{K}\right)-\frac{ru^*}{K}-\frac{v^*\alpha}{\phi_1(\omega)}-\frac{eq}{\phi_2(\omega)}\\
&= -\frac{ru^*}{K};\\
D_{12} &= -\frac{\alpha u^*}{\phi_1(\omega)};\\
D_{21} &= \frac{s\,(v^*)^2\beta}{\left(\dfrac{\beta u}{\phi_1(\omega)}+c\right)^2\phi_1(\omega)};\\
&= \frac{s\beta}{\phi_1(\omega)};\\
D_{22} &= s\left(1-\frac{v^*}{\frac{\beta u^*}{\phi_1(\omega)}+c}\right)-\frac{sv^*}{\frac{\beta u^*}{\phi_1(\omega)}+c}\\
&= -\frac{sv^*}{\frac{\beta u^*}{\phi_1(\omega)}+c}\\
&= -s.
\end{aligned}$$

Note that condition (16) is equivalent to:

$$r>\frac{\alpha c}{\phi_1(\omega)}+\frac{eq}{\phi_2(\omega)},\tag{19}$$

Using (18), we can calculate:

$$Tr(J(E_3(u^*,v^*)))=D_{11}+D_{22}=-\frac{ru^*}{K}-s<0$$

and

$$\begin{aligned}
& Det(J(E_3(u^*,v^*)))\\
=\ & D_{11}D_{22}-D_{12}D_{21}\\
=\ & s\Big(\frac{ru^*}{K}+\frac{\beta}{\phi_1(\omega)}\frac{\alpha u^*}{\phi_1(\omega)}\Big)\\
=\ & s\Big(r-\frac{\alpha v^*}{\phi_1(\omega)}-\frac{eq}{\phi_2(\omega)}+\frac{\beta}{\phi_1(\omega)}\frac{\alpha u^*}{\phi_1(\omega)}\Big)\\
=\ & s\left(r-\frac{\alpha\Big(\dfrac{\beta u^*}{\phi_1(\omega)}+c\Big)}{\phi_1(\omega)}+\frac{eq}{\phi_2(\omega)}-\frac{\beta}{\phi_1(\omega)}\frac{\alpha u^*}{\phi_1(\omega)}\right)
\end{aligned}$$

$$
\begin{aligned}
&= s\left(r - \frac{\alpha c}{\phi_1(\omega)} - \frac{eq}{\phi_2(\omega)}\right) \\
&< 0.
\end{aligned}
$$

Thus, under condition (16), both eigenvalues of the Jacobian matrix $J(E_3(u^*, v^*))$ have negative real parts, which implies that the positive equilibrium $E_3(u^*, v^*)$ is locally asymptotically stable. This completes the proof of Theorem 3.2.

IV. EXTINCTION ANALYSIS

In the previous section, we demonstrated that the boundary equilibrium points E_0 and E_1 are unstable, whereas the boundary equilibrium point E_2 and the positive equilibrium point E_3 are locally asymptotically stable under specific conditions. A natural extension of these results is to explore their global stability properties. In this section, we aim to derive sufficient conditions for the global asymptotic stability of the prey-free equilibrium point $E_2(0, c)$. Specifically, we establish the following result.

Theorem 4.1 *Under the condition (15), the prey-free equilibrium point $E_2(0, c)$ is globally asymptotically stable.*

Proof

For a sufficiently small $\varepsilon > 0$, without loss of generality, we assume:

$$0 < \varepsilon < \frac{\left(\frac{\alpha c}{\phi_1(\omega)} + \frac{eq}{\phi_2(\omega)} - r\right)\phi_1(\omega)}{\alpha}.$$

Under this assumption, inequality (15) implies:

$$r < \frac{\alpha(c-\varepsilon)}{\phi_1(\omega)} + \frac{eq}{\phi_2(\omega)}. \tag{20}$$

From the second equation of system (3) and the positivity of solutions, we derive the following lower bound for the predator population growth:

$$\frac{dv}{dt} = sv\left(1 - \frac{v}{\frac{\beta u}{\phi_1(\omega)} + c}\right) \geq sv\left(1 - \frac{v}{c}\right).$$

Applying Lemma 2.3 from [35] to this inequality, we obtain the asymptotic lower bound for the predator population:

$$\liminf_{t\to+\infty} v(t) \geq c. \tag{21}$$

Furthermore, for any sufficiently small positive constant $\varepsilon > 0$ satisfying $\varepsilon < \frac{c}{2}$, there exists a time $T_1 > 0$ such that for all $t > T_1$, the inequality $v(t) > c - \varepsilon$ holds.

For $t > T_1$, from (20) and the first equation of system (3), we have:

$$
\begin{aligned}
\frac{du}{dt} &= ru\Big(1 - \frac{u}{K}\Big) - \frac{\alpha uv}{\phi_1(\omega)} - \frac{equ}{\phi_2(\omega)} \\
&\leq ru\Big(1 - \frac{u}{K}\Big) - \frac{\alpha u(c-\varepsilon)}{\phi_1(\omega)} - \frac{equ}{\phi_2(\omega)} \\
&< \Big(r - \frac{\alpha(c-\varepsilon)}{\phi_1(\omega)} - \frac{eq}{\phi_2(\omega)}\Big)u,
\end{aligned} \tag{22}
$$

therefore:

$$u(t) < u(T_1)\exp\left[\Big(r - \frac{\alpha u(c-\varepsilon)}{\phi_1(\omega)} - \frac{equ}{\phi_2(\omega)}\Big)(t - T_1)\right]. \tag{23}$$

From this, we can see that as $t \to +\infty$:

$$\lim_{t\to+\infty} u(t) = 0. \tag{24}$$

Equation (24) indicates that there exists $T_2 > T_1$ such that for all $t \geq T_2$, we have:

$$u(t) < \varepsilon. \tag{25}$$

For $t \geq T_2$, from the second equation of system (3) and equation (25), we have:

$$
\begin{aligned}
\tfrac{dv}{dt} &= sv\left(1 - \frac{v}{\frac{\beta u}{\phi_1(\omega)} + c}\right) \\
&\leq sv\left(1 - \frac{v}{\frac{\beta\varepsilon}{\phi_1(\omega)} + c}\right).
\end{aligned} \tag{26}
$$

Applying Lemma 2.3 from [35] to the above inequality, we obtain:

$$\limsup_{t\to+\infty} v(t) \leq \frac{\beta\varepsilon}{\phi_1(\omega)} + c. \tag{27}$$

Since ε is an arbitrarily small positive number, letting $\varepsilon \to 0$ in equation (27), we obtain:

$$\limsup_{t\to+\infty} v(t) \leq c. \tag{28}$$

Combining equations (21) and (28), we have:

$$\lim_{t\to+\infty} v(t) = c. \tag{29}$$

Equations (24) and (29) show that the prey-free equilibrium point $E_2(0, c)$ is globally asymptotically stable. This completes the proof of Theorem 4.1.

V. GLOBAL STABILITY OF THE POSITIVE EQUILIBRIUM POINT $E^* = (u^*, v^*)$

The objective of this section is to conduct a study on the global stability of the positive equilibrium point within system (3). Specifically, we obtain the following result:

Theorem 5.1 *If the following condition holds:*

$$\phi_2(\omega)\, r\phi_1(\omega) > \phi_2(\omega)\,\alpha c + eq\phi_1(\omega) \tag{30}$$

then the positive equilibrium point $E_3(u^*, v^*)$ is globally asymptotically stable. This means that as long as the positive equilibrium point exists, it is globally asymptotically stable.

Proof Previously, we proved that E_0 and E_1 are both unstable. Moreover, under the assumption that condition (30) holds, the proof of Theorem 3.2 shows that the Jacobian matrix of E_2 has a positive eigenvalue, and thus $E_2(0, c)$ is also unstable. To prove that $E_3(u^*, v^*)$ is globally stable, we only need to show that there are no limit cycles in the first quadrant of the system. According to the theory of limit sets in planar systems, all solutions will eventually converge to the positive equilibrium point E_3 as time approaches infinity.

Consider the Dulac function $B(u,v) = u^{-1}v^{-1}$. We can calculate:

$$\begin{aligned}
&\frac{\partial(PB)}{\partial u} + \frac{\partial(QB)}{\partial v}\\
=\ & \frac{r\left(1-\frac{u}{K}\right) - \frac{ru}{K} - \frac{v\alpha}{\phi_1(\omega)} - \frac{qe}{\phi_2(\omega)}}{uv}\\
& - \frac{ru\left(1-\frac{u}{K}\right) - \frac{\alpha uv}{\phi_1(\omega)} - \frac{qeu}{\phi_2(\omega)}}{u^2 v}\\
& - \frac{s}{\left(\frac{\beta u}{\phi_1(\omega)} + c\right) u}\\
=\ & -\frac{K\phi_1(\omega)\, sv + \phi_1(\omega)\, cru + \beta r\, u^2}{uKv\left(c\phi_1(\omega) + \beta u\right)},
\end{aligned} \tag{31}$$

where:

$$\begin{aligned}
P(u,v) &= ru\Big(1-\frac{u}{K}\Big) - \frac{\alpha uv}{\phi_1(\omega)} - \frac{equ}{\phi_2(\omega)},\\
Q(u,v) &= s\left(1 - \frac{v}{\dfrac{\beta u}{\phi_1(\omega)} + c}\right).
\end{aligned} \tag{32}$$

According to the Bendixson-Dulac criterion [36], there are no closed orbits in the first quadrant. Since the solutions of system (3) are bounded and E_3 is the unique positive equilibrium point, it follows that E_3 is globally asymptotically stable.

This completes the proof of Theorem 5.1.

Remark 5.1 Based on Theorem 5.1, we are aware that as soon as the positive equilibrium point comes into existence, it exhibits global asymptotic stability. This, in turn, indicates that within system (3), no bifurcations occur at E_3.

VI. UNIFORM PERSISTENCE

From a biological perspective, if an ecosystem can persist, it means that each population in the system can survive in the long term. In this section, we will use the methods of Jawad et al. [14] and Huang et al. [15] to provide a set of sufficient conditions that ensure the persistence of system (3). In fact, we have the following theorem:

Theorem 6.1 *If the following condition holds:*

$$\phi_2(\omega)\, r\phi_1(\omega) > \phi_2(\omega)\, \alpha c + eq\phi_1(\omega) \tag{33}$$

then system (3) is uniformly persistent.

Proof We have already proven that the system has no limit cycles. Therefore, the limit set of the system can only consist of equilibrium points. If we can show that under the conditions of the theorem, the boundary equilibrium points E_0, E_1, and E_2 cannot be the ω-limit set of system (3), then the trajectories of the system must lie in the interior of the first quadrant, and thus the system is persistent.

Let's consider the persistence function $w(u,v) = u^a v^b$, in which a and b are positive constants. Evidently, for every (u,v) belonging to the positive two-dimensional real-valued space R_2^+, the value of $w(u,v)$ is greater than 0. Moreover, when either u approaches 0 or v approaches 0, the value of $w(u,v)$ approaches 0. Now, we are able to calculate:

$$\begin{aligned}
\Phi(u,v) &= \frac{\dot{w}}{w} = a\Big(r\Big(1-\frac{u}{K}\Big) - \frac{\alpha v}{\phi_1(\omega)} - \frac{eq}{\phi_2(\omega)}\Big)\\
&\quad + b\left(s\Big(1 - \frac{v}{\dfrac{\beta u}{\phi_1(\omega)} + c}\Big)\right).
\end{aligned} \tag{34}$$

From this, we can calculate for all $a, b > 0$:

$$\begin{aligned}
\Phi(E_0) &= a\Big(r - \frac{eq}{\phi_2(\omega)}\Big) + bs > 0,\\
\Phi(E_1) &= bs > 0,\\
\Phi(E_2) &= a\Big(r - \frac{\alpha c}{\phi_1(\omega)} - \frac{eq}{\phi_2(\omega)}\Big) > 0,
\end{aligned} \tag{35}$$

Equations (35) indicate that E_0, E_1, and E_2 cannot serve as the limit set of system (3). Utilizing Gard's method, as presented in [37], it can be concluded that system (3) is persistent.

VII. THE IMPACT OF WIND EFFECTS

Jawad et al. [17] and Huang et al. Huang et al[18] both assumed that the wind effect is modeled as $1+\omega$, where ω represents the strength of the wind. However, we believe this is not entirely reasonable, as it does not account for the different impacts of wind on predator foraging and human harvesting. Therefore, we introduced $\phi_1(\omega) = 1 + k_1\omega$ and $\phi_2(\omega) = 1 + k_2\omega$, where k_1 and k_2 are positive constants. Clearly, when the two populations coexist, their final densities will be influenced by k_1 and k_2. Therefore, it is crucial to investigate the interplay between these parameters to better understand their influence on the system dynamics.

This section provides a detailed exploration of the relationship between u^*, v^*, and k_1, k_2.

A. *Relationship between u^* and k_1*

First, from equation (10), u^* can be expressed as:

$$u^* = \frac{N(k_1)}{D(k_1)},$$

where:

$$\begin{aligned}
N(k_1) &= -(1+k_1\omega)K\Big[(1+k_2\omega)\alpha c\\
&\qquad -(1+k_2\omega)r(1+k_1\omega)\\
&\qquad + eq(1+k_1\omega)\Big],\\
D(k_1) &= (1+k_2\omega)\left[K\alpha\beta + r(1+k_1\omega)^2\right].
\end{aligned} \tag{36}$$

Thus, we have:

$$\frac{\partial u^*}{\partial k_1} = \frac{D(k_1)\frac{\partial N(k_1)}{\partial k_1} - N(k_1)\frac{\partial D(k_1)}{\partial k_1}}{D(k_1)^2}. \tag{37}$$

Note that:

$$\begin{aligned}
&\tfrac{\partial N(k_1)}{\partial k_1}\\
= \;& -\omega K\Big[(1+k_2\omega)\alpha c-(1+k_2\omega)r(1+k_1\omega)\\
&\quad +eq(1+k_1\omega)\Big]\\
&-(1+k_1\omega)K\left[-(1+k_2\omega)r\omega+eq\omega\right]\\
= \;& -\omega K(1+k_2\omega)\alpha c+\omega K(1+k_2\omega)r(1+k_1\omega)\\
&-\omega Keq(1+k_1\omega)+(1+k_1\omega)K(1+k_2\omega)r\omega\\
&-(1+k_1\omega)Keq\omega\\
= \;& -\omega K(1+k_2\omega)\alpha c+2\omega K(1+k_2\omega)r(1+k_1\omega)\\
&-2\omega Keq(1+k_1\omega).
\end{aligned} \tag{38}$$

and:

$$\begin{aligned}
\tfrac{\partial D(k_1)}{\partial k_1} &= (1+k_2\omega)\left[2r(1+k_1\omega)\omega\right]\\
&= 2\omega r(1+k_2\omega)(1+k_1\omega).
\end{aligned} \tag{39}$$

Substituting $\frac{\partial N(k_1)}{\partial k_1}$ and $\frac{\partial D(k_1)}{\partial k_1}$ into equation (36), we have:

$$\frac{\partial u^*}{\partial k_1}=\frac{(1+k_2\omega)\left[K\alpha\beta+r(1+k_1\omega)^2\right]A_1-B_1}{(1+k_2\omega)^2\left[K\alpha\beta+r(1+k_1\omega)^2\right]^2}, \tag{40}$$

where:

$$\begin{aligned}
A_1 &= -\omega K(1+k_2\omega)\alpha c+2\omega K(1+k_2\omega)r(1+k_1\omega)\\
&\quad -2\omega Keq(1+k_1\omega),\\
B_1 &= N(k_1)\left[2\omega r(1+k_2\omega)(1+k_1\omega)\right].
\end{aligned}$$

Since the denominator of equation (40) is always positive, we only need to analyze the sign of the numerator. Note that under the condition for the existence of the positive equilibrium point, $N_1(k_1)>0$. Therefore, the sign of the numerator is mainly determined by:

$$\begin{aligned}
\Delta = \;& -\omega K(1+k_2\omega)\alpha c\\
&+2\omega K(1+k_2\omega)r(1+k_1\omega)\\
&-2\omega Keq(1+k_1\omega).
\end{aligned} \tag{41}$$

By applying the condition for the existence of the positive equilibrium point, it can be readily verified that:

$$\Delta>0. \tag{42}$$

This implies:

$$\frac{\partial u^*}{\partial k_1}>0. \tag{43}$$

In other words, u^* is a monotonically increasing function of k_1.

From an ecological perspective, this conclusion is easy to understand. As k_1 increases, $\phi_1(\omega)=1+k_1\omega$ increases, which reduces the search efficiency of predators. This decreases the predation pressure on prey, leading to an increase in the prey population density u^*. In other words, the negative impact of wind on predator search efficiency results in an increase in prey density.

B. *Relationship between v^* and k_1*

Note that v^* is expressed as:

$$v^*=\frac{\beta u^*}{\phi_1(\omega)}+c,$$

where $\phi_1(\omega)=1+k_1\omega$.

Using the chain rule, the partial derivative of v^* with respect to k_1 is:

$$\frac{\partial v^*}{\partial k_1}=\frac{\beta\frac{\partial u^*}{\partial k_1}\phi_1(\omega)-\beta u^*\omega}{\phi_1(\omega)^2}. \tag{44}$$

Since $\frac{\partial u^*}{\partial k_1}>0$, the first term $\beta\frac{\partial u^*}{\partial k_1}\phi_1(\omega)$ is positive. The second term $-\beta u^*\omega$ is negative. Therefore, the sign of the numerator depends on the relative magnitudes of these two terms. As k_1 increases, $\phi_1(\omega)$ increases, reducing the search efficiency of predators and decreasing the predation pressure on prey, which leads to an increase in prey density. However, the increase in $\phi_1(\omega)$ may also cause $\frac{\partial u^*}{\partial k_1}\phi_1(\omega)$ to decrease. Overall, the change in v^* depends on the relative changes in u^* and $\phi_1(\omega)$. If the increase in u^* is not sufficient to offset the increase in $\phi_1(\omega)$, then v^* will decrease. Specifically, when $\frac{\partial u^*}{\partial k_1}\phi_1(\omega)<\beta u^*\omega$, we have $\frac{\partial v^*}{\partial k_1}<0$, meaning v^* is a monotonically decreasing function of k_1. Conversely, if $\frac{\partial u^*}{\partial k_1}\phi_1(\omega)>\beta u^*\omega$, then $\frac{\partial v^*}{\partial k_1}>0$, meaning v^* is a monotonically increasing function of k_1.

From an ecological perspective, as the search efficiency of predators decreases, the density of prey increases. As the number of prey increases, the density of the predator population also increases. However, the increase in prey density is limited. Beyond a certain point, as wind effects further increase, the ability of predators to capture prey decreases, ultimately leading to a gradual decrease in the final density of the predator population.

C. *Relationship between u^* and k_2*

First, from equation (10), u^* can be expressed as:

$$u^*=\frac{(k_1\omega+1)\,KC_1(k_2)}{(k_2\omega+1)\left(K\alpha\beta+r\,(k_1\omega+1)^2\right)},$$

where:

$$\begin{aligned}
C_1(k_2) = \;& \Big((k_2\omega+1)\,\alpha c\\
&-(k_2\omega+1)\,r\,(k_1\omega+1)\\
&+eq\,(k_1\omega+1)\Big).
\end{aligned} \tag{45}$$

Thus, we have:

$$\begin{aligned}
\frac{\partial u^*}{\partial k_2} = \;& \frac{(k_1\omega+1)\,K\,(\omega\alpha c-\omega r\,(k_1\omega+1))}{(k_2\omega+1)\left(K\alpha\beta+r\,(k_1\omega+1)^2\right)}\\
&+\frac{(k_1\omega+1)\,KC_2(k_2)\omega}{(k_2\omega+1)^2\left(K\alpha\beta+r\,(k_1\omega+1)^2\right)}\\
= \;& \frac{(k_1\omega+1)^2\,K\omega eq}{(k_2\omega+1)^2\left(K\alpha\beta+r\,(k_1\omega+1)^2\right)}\\
> \;& 0.
\end{aligned} \tag{46}$$

This shows that u^* is a monotonically increasing function of k_2. From an ecological perspective, as the impact of wind increases, humans expend the same effort but harvest fewer fish, which benefits the survival of the fish population.

D. Relationship between v^* and $k_2\omega$

From equation (10), the expressions for u^* and v^* are:

$$v^* \;=\; \frac{(k_1\omega+1)H}{(k_2\omega+1)\left(K\alpha\beta+r(k_1\omega+1)^2\right)}, \tag{47}$$

where

$$\begin{aligned} H \;&\overset{\text{def}}{=}\; K\left(k_2\omega+1\right)\beta r - K\beta eq \\ &\quad +c\left(k_1\omega+1\right)\left(k_2\omega+1\right)r. \end{aligned} \tag{48}$$

Thus, we have:

$$\begin{aligned} &\frac{\partial v^*}{\partial k_2} \\ =\;& \frac{\left(k_1\omega+1\right)\left(K\omega\beta r+c\left(k_1\omega+1\right)\omega r\right)}{\left(k_2\omega+1\right)\left(K\alpha\beta+r\left(k_1\omega+1\right)^2\right)} \\ &-\frac{\left(k_1\omega+1\right)H\omega}{\left(k_2\omega+1\right)^2\left(K\alpha\beta+r\left(k_1\omega+1\right)^2\right)} \\ =\;& \frac{\left(k_1\omega+1\right)\omega K\beta eq}{\left(k_2\omega+1\right)^2\left({k_1}^2\omega^2 r+K\alpha\beta+2k_1\omega r+r\right)} \\ >\;& 0 \end{aligned} \tag{49}$$

This shows that v^* is a monotonically increasing function of $k_2\omega$. From an ecological perspective, as the impact of wind increases, human harvesting decreases, which benefits the growth of the prey population. As the prey population grows, the food available to the predator population increases, ultimately leading to an increase in the density of the predator population.

E. Impact of wind effect ω on the positive equilibrium point

Theorem 4.1 in Huang et al. [18] shows that when $\omega = 0$ (i.e., no wind), if the following condition holds:

$$r < \alpha c + eq \tag{50}$$

Consequently, the prey-free equilibrium point $E_2(0, c)$ is asymptotically stable on a global scale, meaning the prey species goes extinct. Note that condition (9) is equivalent to:

$$r > \frac{\alpha c}{\phi_1(\omega)} + \frac{eq}{\phi_2(\omega)} \tag{51}$$

As ω approaches infinity, both $\phi_1(\omega)$ and $\phi_2(\omega)$ approach infinity. This implies that as long as ω is sufficiently large, condition (51) will necessarily hold. In other words, when the wind speed is sufficiently high, the system will necessarily have a positive equilibrium point. Theorem 5.1 has already shown that the existence of a positive equilibrium point implies local asymptotic stability. This indicates that wind effects can effectively increase the probability of coexistence between the two populations, contributing to the stability of the ecosystem.

As the wind speed ω increases, $\phi_1(\omega)$ increases, meaning the search efficiency of predators decreases. This reduces the predation efficiency of predators on prey, potentially increasing the prey population density u^*. As the wind speed ω increases, $\phi_2(\omega)$ also increases, meaning the efficiency of human harvesting decreases. This reduces the impact of human harvesting on prey, potentially increasing the prey population density u^*.

When ω approaches infinity, from the proof of Theorem 4.1, we know that $\lim_{t\to+\infty} v(t) \geq c$. In other words, the density of the predator population will eventually be no less than c. Note that $\frac{\alpha c}{\phi_1(\omega)} \to 0$ and $\frac{eq}{\phi_2(\omega)} \to 0$. This means that as ω approaches infinity, the limiting equation of the first equation in system (3) is:

$$\frac{du}{dt} \;=\; ru\Big(1-\frac{u}{K}\Big), \tag{52}$$

Thus, as $t \to +\infty$, we have $\lim_{t\to+\infty} u(t) = K$. In other words, if the wind is sufficiently strong, the impact of the predator population and human harvesting on the prey population becomes negligible, and the prey population density eventually approaches its environmental carrying capacity.

F. Impact of other food resources

From equation (10), what the expressions of u^* and v^* reveal is that other food sources play a crucial part in the system's persistence and stability. After calculation, we get:

$$\frac{du^*}{dc} = -\frac{\left(k_1\omega+1\right)K\alpha}{K\alpha\beta+r\left(k_1\omega+1\right)^2} < 0,$$

$$\frac{dv^*}{dc} = \frac{\left(k_1\omega+1\right)^2 r}{K\alpha\beta+r\left(k_1\omega+1\right)^2} > 0.$$

As other food resources increase, the density of the predator species increases. As the predator population grows, the demand for food also increases, ultimately leading to a decrease in the density of the prey population.

VIII. DYNAMICAL BEHAVIORS UNDER EXTREME SCENARIOS

A. Windless environment ($\omega \to 0$)

When wind speed approaches zero, the system reduces to the classical Leslie-Gower model:

$$\begin{aligned} \tfrac{du}{dt} \;&=\; ru\left(1-\tfrac{u}{K}\right)-\alpha uv-equ, \\ \tfrac{dv}{dt} \;&=\; sv\left(1-\tfrac{v}{\beta u+c}\right). \end{aligned} \tag{53}$$

Equilibrium Stability:

- *Prey-free equilibrium $E_2(0, c)$:* Globally stable if $r < \alpha c + eq$.
- *Positive equilibrium $E_3(u^*, v^*)$:* Exists and is globally stable if $r > \alpha c + eq$.

B. Extreme wind speed ($\omega \to \infty$)

Under extremely high wind speeds, the system decouples approximately:

$$\begin{aligned} \tfrac{du}{dt} \;&\approx\; ru\left(1-\tfrac{u}{K}\right), \\ \tfrac{dv}{dt} \;&\approx\; sv\left(1-\tfrac{v}{c}\right). \end{aligned} \tag{54}$$

Equilibrium Analysis:

- *New equilibrium $E_4(K, c)$:* Eigenvalues $\lambda_1 = -r/K$, $\lambda_2 = -s/c$ indicate a stable node.
- *Ecological implication:* Prey density approaches carrying capacity K, while predators rely on external food source c.

C. Mutation phenomena near critical wind speed

Saddle-node bifurcation mechanism: At critical wind speed ω_c satisfying:

$$r = \frac{\alpha c}{k_1 \omega_c} + \frac{eq}{k_2 \omega_c},$$

the positive equilibrium E_3 collides with the boundary equilibrium E_2, triggering a dynamical phase transition.

D. Lyapunov exponent analysis

A: Calculation Method

1. Jacobian linearization:

$$J = \begin{pmatrix} \partial f/\partial u & \partial f/\partial v \\ \partial g/\partial u & \partial g/\partial v \end{pmatrix}. \tag{55}$$

2. Eigenvalue solving:

$$\lambda_{1,2} = \frac{Tr(J) \pm \sqrt{Tr(J)^2 - 4Det(J)}}{2}.$$

3. Maximum Lyapunov exponent: $\lambda_{\max} = \max(Re(\lambda_1), Re(\lambda_2))$.

B: Exponent Variation Rules

TABLE I

VARIATION OF LYAPUNOV EXPONENTS WITH WIND SPEED

Wind Speed Range	Dominant Equilibrium	$\lambda_{\max}$ Sign
$\omega < \omega_c$	E_3	Negative
$\omega = \omega_c$	Bifurcation point	Zero
$\omega > \omega_c$	E_2	Negative

E. Ecological management implications

- **Critical wind speed threshold:** Set ω_c as the upper fishing ban threshold in fishery policies.
- **Adaptive management:** Monitor population density mutation risks when $\omega > \omega_{opt}$ (optimal wind speed for peak predator density).
- **Climate change adaptation:** Dynamically adjust management strategies as long-term wind distribution shifts alter bifurcation thresholds.

IX. NUMERICAL SIMULATIONS

Example 9.1

Now, let's conduct a study on the following model:

$$\begin{aligned} \frac{du}{dt} &= u\Big(1 - \frac{u}{10}\Big) - \frac{uv}{1 + 0.1 \times \omega} \\ &\quad - \frac{0.5u}{1 + 0.1 \times 5}, \\ \frac{dv}{dt} &= v\left(1 - \frac{v}{\dfrac{u}{1 + 0.1 \times \omega} + 2}\right). \end{aligned} \tag{56}$$

In this model, when compared with system (3), we set $r = 1$, $K = 10$, $\alpha = 1$, $e = 0.5$, $q = 1$, $s = 1$, $\beta = 1$, $c = 2$, $k_1 = 0.1$ and $k_2 = 0.1$.

(1) Take ω as the bifurcation parameter. Since $r = 1 < \alpha c + eq = 2.5$, from the continuity of the function, for ω not so large, $r < \frac{\alpha c}{\phi_1(\omega)} + \frac{eq}{\phi_2(\omega)}$, it follows from Theorem 3.1 that the system has no positive equilibrium. However, as $\omega \to +\infty$, $r > \frac{\alpha c}{\phi_1(\omega)} + \frac{eq}{\phi_2(\omega)}$ always holds, consequently, system admits a unique positive equilibrium. Fig 1-2 confirms this observation. From Figure 1 and 2, one could see that the critical value of wind effect is $w_c \approx 1$.

(2) Take $\omega = 5$. In this case, simple calculation shows that

$$r = 1 < \frac{2.5}{1.5} = \frac{\alpha c}{\phi_1(\omega)} + \frac{eq}{\phi_2(\omega)}. \tag{57}$$

According to Theorem 4.1, the prey-free equilibrium point $E_2(0, 2)$ is globally asymptotically stable. Fig 3 and 4 are the time series solution of $u(t)$ and $v(t)$, Fig.5 is the phase ortrait of the system (56), they all support the assertion.

Example 9.2 Let us now study the following model:

$$\begin{aligned} \frac{du}{dt} &= 2u\Big(1 - \frac{u}{10}\Big) - \frac{uv}{1 + 0.1 \times 5} \\ &\quad - \frac{0.2u}{1 + 0.1 \times 5}, \\ \frac{dv}{dt} &= v\left(1 - \frac{v}{\dfrac{u}{1 + 0.1 \times 5} + 1}\right). \end{aligned} \tag{58}$$

Here, corresponding to system (3), we take $r = 2$, $K = 10$, $\alpha = 1$, $e = 0.2$, $q = 1$, $s = 1$, $\beta = 1$, $c = 1$, $k_1 = 0.1$, $k_2 = 0.1$, and $\omega = 5$. Note that:

$$\phi_1(\omega) = 1 + k_1\omega = 1 + 0.1 \times 5 = 1.5$$

$$\phi_2(\omega) = 1 + k_2\omega = 1 + 0.1 \times 5 = 1.5$$

Thus, we have:

$$\phi_2(\omega) r \phi_1(\omega) = 1.5 \times 2 \times 1.5 = 4.5$$

$$\begin{aligned} & \phi_2(\omega)\alpha c + eq\phi_1(\omega) \\ = \;& 1.5 \times 1 \times 1 + 0.2 \times 1 \times 1.5 \\ = \;& 1.5 + 0.3 = 1.8 \end{aligned}$$

Clearly, the following condition holds:

$$\phi_2(\omega) r \phi_1(\omega) > \phi_2(\omega)\alpha c + eq\phi_1(\omega)$$

Therefore, the conditions of Theorem 5.1 are satisfied, and the positive equilibrium point $E_3(u^*, v^*) \approx (1.862, 2.241)$ is globally asymptotically stable. The numerical simulations (Figures 6-9) support this conclusion. Here Fig. 6 and 7 are the time series solution of $u(t)$ and $v(t)$, respectively. Fig. 8 is the phase ortrait of the system (58), Fig.9 shows the solutions from 3D-space.

Example 9.3 Consider the following model:

$$\begin{aligned} \frac{du}{dt} &= 2u\Big(1 - \frac{u}{10}\Big) - \frac{uv}{1 + 0.1 \times \omega} - \frac{0.2u}{1 + 0.1 \times \omega}, \\ \frac{dv}{dt} &= v\left(1 - \frac{v}{\dfrac{u}{1 + 0.1 \times \omega} + 1}\right). \end{aligned} \tag{59}$$

In this context, in relation to system (3), we set $r = 2$, $K = 10$, $\alpha = 1$, $e = 0.2$, $q = 1$, $s = 1$, $\beta = 1$, $c = 1$, $k_1 = 0.1$, and $k_2 = 0.1$. We vary ω as $\omega = 0, 5, 10, 1000$, with the initial condition $(u(0), v(0)) = (1, 1)$. Figures 10, 11 and 12 illustrate the behavior of the system's solutions for different values of ω. It can be observed that as ω increases, the value of u^* also increases. When ω is large enough, $u(t) \to K$ and $v(t) \to c$. This result is in line with the theoretical analysis presented in Section 7.6. Additionally, Figure 5 shows that as ω increases from 0 to ∞, the density of the predator population first increases, then decreases, and finally approaches c as the wind effect becomes strong enough.

Example 9.4 Consider the following model:

$$\begin{aligned} \frac{du}{dt} &= 2u\Big(1-\frac{u}{10}\Big) - \frac{uv}{1+k_1\times 5} - \frac{0.2u}{1+k_2\times 5}, \\ \frac{dv}{dt} &= v\left(1 - \frac{v}{\dfrac{u}{1+k_1\times 5}+1}\right). \end{aligned} \tag{60}$$

Here, corresponding to system (3), we take $r = 2$, $K = 10$, $\alpha = 1$, $e = 0.2$, $q = 1$, $s = 1$, $\beta = 1$, $c = 1$, and $\omega = 5$.

(1) Take $k_2 = 0.1$, then as k_1 varies, u^* and v^* also vary. Figure 13 shows their relationship. It can be seen that u^* is a monotonically increasing function of k_1, while v^* first increases monotonically and then decreases monotonically. Finally, as $k_1 \to +\infty$, $v^* \to c$. This is consistent with the theoretical analysis in Sections 7.1 and 7.2.

(2) Take $k_1 = 0.1$, as k_2 varies, u^* also varies. Figure 14 shows their relationship. It can be seen that u^* is a monotonically increasing function of k_2. This is consistent with the theoretical analysis in Sections 7.3 and 7.4.

(3) Both k_1 and k_2 varies, in this case, u^* and v^* also varies. Figure 15 and 16 show the relationship among u^*, v^* and k_1, k_2. It can be seen that u^* is a monotonically increasing function of k_1 and k_2.

This is consistent with the theoretical analysis in Sections 7.3 and 7.4.

Example 9.5 Consider the following model:

$$\begin{aligned} \frac{du}{dt} &= u\Big(1-\frac{u}{10}\Big) - \frac{2uv}{1+0.1\times\omega} - \frac{0.5u}{1+k_2\times\omega}, \\ \frac{dv}{dt} &= v\left(1 - \frac{v}{\dfrac{u}{1+0.1\times 5}+1}\right). \end{aligned} \tag{61}$$

Here, corresponding to system (3), we take $r = 1$, $K = 10$, $\alpha = 1$, $e = 0.5$, $q = 1$, $s = 1$, $\beta = 1$, $c = 1$ and $k_1 = 0.1$. For the system without harvesting and wind effect,

$$r = 1.1 > 1 = \alpha c. \tag{62}$$

In this case, the system admits a unique positive equilibrium, which is globally asymptotically stable. However, for the system with harvesting and without wind effect,

$$r = 1.1 < 1.5 = \alpha c + eq, \tag{63}$$

then, the prey species will be driven to extinction. That is, with the human harvesting, the prey species will finally be driven to extinction. Now, if we further incorporating the wind effect to the system, obviously, for ω enough large,

$$r = 1.1 > \frac{\alpha c}{\phi_1(\omega)} + \frac{eq}{\phi_2(\omega)}. \tag{64}$$

Then the system again admits a unique positive equilibrium which is globally asymptotically stable. Fig. 17 and 18 show this phenomenon. The wind effect plays a crucial role in the long-term survival of the prey population by reducing the intensity of human harvesting.

X. CONCLUSION AND FUTURE PERSPECTIVES

A. Theoretical Contributions

This paper breaks through the limitations of traditional single-factor models by introducing a dual-channel wind effect framework that simultaneously incorporates the impact of wind on natural predation and human harvesting. Specifically, we quantify the dynamic effects of wind speed on predator search efficiency and human harvesting intensity through the nonlinear functions $\phi_1(\omega) = 1 + k_1\omega$ (predation efficiency suppression term) and $\phi_2(\omega) = 1 + k_2\omega$ (harvesting intensity attenuation term). Numerical simulations validate the following critical phenomenon:

$$\lim_{\omega\to\infty} u(t) = K, \quad \lim_{\omega\to\infty} v(t) = c,$$

revealing that under extreme wind speeds, prey populations asymptotically approach environmental carrying capacity, while predators rely on external food sources. This finding highlights critical ecological phenomena under extreme climatic conditions.

Furthermore, we establish the necessary and sufficient condition for global asymptotic stability:

$$\phi_2(\omega) r \phi_1(\omega) > \phi_2(\omega)\alpha c + eq\phi_1(\omega),$$

proving that the existence of a positive equilibrium directly guarantees global convergence, thereby quantifying ecosystem resilience.

B. Ecological Implications

Our study reveals the profound impact of wind speed on population dynamics, particularly when wind speed exceeds a critical threshold ($\omega > \omega_c$). The synergistic effects of declining predation efficiency ($\partial\phi_1/\partial\omega$) and harvesting attenuation ($\partial\phi_2/\partial\omega$) can break prey extinction thresholds. This finding provides important guidance for biodiversity conservation in climate-sensitive regions.

Additionally, we uncover parameter sensitivity rules: predator density v^* exhibits **unimodal variation** with wind speed (peak density corresponds to optimal wind speed ω_{opt}), while prey density u^* remains positively correlated with the harvesting interference coefficient k_2. These results offer a theoretical foundation for defining ”no-fishing wind speed intervals” in fisheries management.

C. Validation through Numerical Simulations

Through extensive numerical simulations, we validate the theoretical analysis and further elucidate the specific effects of wind speed on population dynamics. For instance, when wind speed is low, prey populations may face extinction due to predation pressure and human harvesting. However, as wind speed increases, the decline in predation efficiency and the attenuation of harvesting intensity allow prey populations to recover and eventually approach environmental carrying capacity. This phenomenon is particularly pronounced under extreme wind speeds, indicating that wind plays a critical role in ecosystem stability.

Moreover, the simulations reveal non-monotonic variation in predator density: as wind speed increases, predator density first increases and then decreases, eventually stabilizing at c. This finding provides important insights for fisheries management: when formulating harvesting policies, the impact of wind speed on both predator and prey populations must be carefully considered to avoid ecosystem imbalance caused by overharvesting.

D. Future Research Directions

1. **Asymmetric Wind Effect Scenarios**: Future research could explore nonlinear forms of $\phi_1(\omega)$ and $\phi_2(\omega)$ (e.g., exponential or threshold-dependent) to investigate their bifurcation impacts on system dynamics.
2. **Climate-Coupled Stochastic Models**: Incorporating stochastic wind fluctuations (e.g., $\omega(t) = \omega_0 + \sigma W_t$, where W_t is a Wiener process) to assess ecological risks under extreme climate events.
3. **Empirical Validation**: Calibrating $\phi_1(\omega)$ and $\phi_2(\omega)$ using remote-sensing wind data and fishery statistics to verify the biological plausibility of the model and provide more precise guidance for real-world ecosystem management.

E. Ecological Management Recommendations

Based on our findings, we propose the following ecological management recommendations:

1. **Set Critical Wind Speed Thresholds**: Use ω_c as the upper limit for fishing bans in fisheries policies to protect prey populations from overharvesting.
2. **Adaptive Management**: Monitor risks of population density mutations when wind speed exceeds the optimal value ω_{opt}, and adjust harvesting strategies accordingly.
3. **Climate Change Adaptation**: Dynamically adapt management strategies in response to long-term shifts in wind speed distributions to mitigate the potential impacts of climate change on ecosystem stability.

ACKNOWLEDGMENT

The authors wish to convey their thanks to Dr. Shireen Jawad for the communication.

This exchange drew our intense attention to the wind effect and inspired us to conduct relevant research.

REFERENCES

[1] X. Wang, L. Zanette, X. Zou, "Modelling the fear effect in predator-prey interactions," *Journal of Mathematical Biology,* vol.73, no. 5, pp. 1179-1204, 2016.

[2] X. Wang, X. Zou, "Modeling the fear effect in predator-prey interactions with adaptive avoidance of predators, Bulletin of Mathematical Biology, 2017, vol. 79, no. 6, pp. 1325-1359, 2017.

[3] K. Kundu, S. Pal and S. Samanta, "Impact of fear effect in a discrete-time predator-prey system, " *Bull. Calcuta Math. Soc,* vol. 110, no.3, pp. 245-264, 2019.

[4] S. K. Sasmal, "Population dynamics with multiple Allee effects induced by fear factors-A mathematical study on prey-predator interactions," *Applied Mathematical Modelling,* vol. 64, no.1, pp. 1-14, 2018.

[5] K. Fang, Z. Zhu, F. Chen, et al. "Qualitative and bifurcation analysis in a Leslie-Gower model with Allee effect," *Qualitative Theory of Dynamical Systems,* vol. 21, no.3, Article ID 86, 2022.

[6] X. Lin, X. Xie, et al, "Convergences of a stage-structured predator-prey model with modified Leslie-Gower and Holling-type II schemes," *Advances in Difference Equations,* 2016, 2016, Article ID 181.

[7] Z. Xiao, Z. Li, Z. Zhu, et al. "Hopf bifurcation and stability in a Beddington-DeAngelis predator-prey model with stage structure for predator and time delay incorporating prey refuge," *Open Mathematics,* vol. 17, no.1, pp. 141-159, 2019.

[8] Q. Yue, "Permanence of a delayed biological system with stage structure and density-dependent juvenile birth rate," *Engineering Letters,* vol. 27. no.2, pp. 263-268, 2019.

[9] X. Xie, Y. Xue, et al. "Permanence and global attractivity of a nonautonomous modified Leslie-Gower predator-prey model with Holling-type II schemes and a prey refuge,"*Advances in Difference Equations,* 2016, 2016, Article ID 184.

[10] H. Deng, F. Chen, Z. Zhu, et al, "Dynamic behaviors of Lotka-Volterra predator-prey model incorporating predator cannibalism," *Advances in Difference Equations,* 2019, Article ID 359.

[11] F. D. Chen, Q. X. Lin, X. D. Xie, et al, "Dynamic behaviors of a nonautonomous modified Leslie-Gower predator-prey model with Holling-type III schemes and a prey refuge," *Journal of Mathematics and Computer Science,* vol.17, no.2, pp. 266-277, 2017.

[12] F. Chen, X. Guan, X. Huang, et al. "Dynamic behaviors of a Lotka-Volterra type predator-prey system with Allee effect on the predator species and density dependent birth rate on the prey species," *Open Mathematics,* vol.17, no.1, pp.1186-1202, 2019.

[13] Z. W. Xiao, Z. Li, "Stability analysis of a mutual interference predator-prey model with the fear effect," *Journal of Applied Science and Engineering,* vol. 22, no.2, pp. 205-211, 2019.

[14] W. Yin, Z. Li, F. Chen, et al. "Modeling Allee effect in the Leslie-Gower predator-prey system incorporating a prey refuge," *International Journal of Bifurcation and Chaos,* vol.32, no.06, Article ID 2250086, 2022.

[15] Z. Zhu, Y. Chen, Z. Li, et al. "Stability and bifurcation in a Leslie-Gower predator-prey model with Allee effect," *International Journal of Bifurcation and Chaos,* vol.32, no.03, Article ID: 2250040, 2022.

[16] E. Klimczuk, L. Halupka, B. Czyz, et al. "Factors driving variation in biparental incubation behaviour in the reed warbler Acrocephalus scirpaceus, " *Ardea*, vol.103, no.1, pp.51-59, 2015.

[17] S. Jawad, D. Sultan, M. Winter, "The dynamics of a modified Holling-Tanner prey-predator model with wind effect, " *International Journal of Nonlinear Analysis and Applications*, vol. 12(Special Issue): pp. 2203-2210, 2021.

[18] C. Huang, F. Chen, Q. Zhu, et al. "How the wind changes the Leslie-Gower predator-prey system," *IAENG International Journal of Applied Mathematics*, vol. 53, no.3, pp. 907-915, 2023.

[19] M. J. Cherry, B .T. Barton, "Effects of wind on predator-prey interactions, " *Food Webs*, vol.13, no.1, pp. 92-97, 2017.

[20] S. L. Lima, L. M. Dill, " Behavioral decisions made under the risk of predation: a review and prospectus, " *Canadian journal of zoology*, vol.68, no.4, pp. 619-640, 1990.

[21] B. P. Kotler, J. S. Brown, O. Hasson, "Factors affecting gerbil foraging behavior and rates of owl predation, " *Ecology*, vol.72, no.6, pp. 2249-2260, 1991.

[22] A .J. Wirsing, K. E. Cameron, M. R. Heithaus, "Spatial responses to predators vary with prey escape mode, " *Animal Behaviour*, vol.79, no.3, pp. 531-537, 2010.

[23] P. E. Stander, I. I. Ghau, D. Tsisaba, et al. "Tracking and the interpretation of spoor: a scientifically sound method in ecology, " *Journal of Zoology*, vol. 242, no. 2, pp. 329-341, 1997.

[24] J. J. Magnuson, L. B. Crowder, P. A. Medvick, "Temperature as an ecological resource, " *American Zoologist*, vol.19, no.1, pp. 331-343, 1979.

[25] L. R. Taylor, "Insect migration, flight periodicity and the boundary layer, " *The Journal of Animal Ecology*, vol.43, no.1, pp. 225-238, 1974.

[26] B. Ruderer, T. Alerstam, "Bird Migration," Cambridge University Press, Cambridge, New York, Melbourne, 1990.

[27] R. E. Johannes, “Words of the Lagoon: Fishing and Marine Lore in the Palau District of Micronesia,” University of California Press, 1981.

[28] M. A. Aziz-Alaoui, M. Daher Okiye, “Boundedness and global stability for a predator-prey model with modified Leslie-Gower and Holling-type II schemes.” *Applied Mathematics Letters,* vol. 16, no.7, pp.1069-1075, 2003.

[29] P. H. Leslie, “A stochastic model for studying the properties of certain biological systems by numerical methods,” *Biometrika*, vol. 45, no.1, pp. 16-31, 1958.

[30] A. Korobeinikov, “A Lyapunov function for Leslie-Gower predator-prey models,” *Applied Mathematics Letters*, vol.14, no.3, pp. 697-699, 2001.

[31] M. J. Cherry, B. T. Barton, “Effects of wind on predator-prey interactions, ” *Food Webs,* vol.13, no.1, pp. 92-97, 2017.

[32] D. Barman, V. Kumar, J. Roy, et al. “Modeling wind effect and herd behavior in a predator-prey system with spatiotemporal dynamics, ” *The European Physical Journal Plus*, vol.137, no.8, 950-960, 2022.

[33] D. Barman, J. Roy, S. Alam, “Impact of wind in the dynamics of prey-predator interactions,” *Mathematics and Computers in Simulation*, vol.191, no.1, pp. 49-81, 2022.

[34] P. Panja, “Impacts of wind and anti-predator behaviour on predator-prey dynamics: a modelling study,” *International Journal of Computing Science and Mathematics*, vol.15, no.4, pp. 396-407, 2022.

[35] F. Chen, Z. Li, Y. Huang. “Note on the permanence of a competitive system with infinite delay and feedback controls, ” *Nonlinear Analysis: Real World Applications*, vol.8, no.2, pp. 680-687, 2007.

[36] Y. C. Zhou, Z. Jin, J. L. Qin, “Ordinary Differential Equation and Its Application,” Beijing, Science Press, 2003.

[37] T. C. Gard and T. G. Hallam, “Persistence in food webs-I Lotka-Volterra food chains,” *Bull. Math. Biol.* vol.41, no.6, pp. 877-891, 1979.

[38] K. Fang, J. Chen, Z. Zhu, et al. “Qualitative and bifurcation analysis of a single species Logistic model with Allee effect and feedback control,” *IAENG International Journal of Applied Mathematics*, vol. 52, no. 2, pp. 320-326, 2022.

[39] F. Chen, S. Lin, S. Chen, et al. “Global stability of Leslie-Gower predator-prey model with density dependent birth rate on prey species and prey refuge, ” *WSEAS Transactions on Systems and Control*, vol.22, no.1, pp 41-48, 2023.

[40] Z. Zhu, R. Wu, F. Chen, et al. “Dynamic behaviors of a Lotka-Volterra commensal symbiosis model with non-selective Michaelis-Menten type harvesting,” *IAENG International Journal of Applied Mathematics*, vol. 50, no.2, pp.396-404, 2020.

[41] X. R. Li, Q. Yue, F. D. Chen, “The dynamic behaviors of nonselective harvesting Lotka-Volterra predator-prey system with partial closure for populations and the fear effect of the prey species,” *IAENG International Journal of Applied Mathematics*, vol. 53, no. 3, pp. 818-825, 2023.

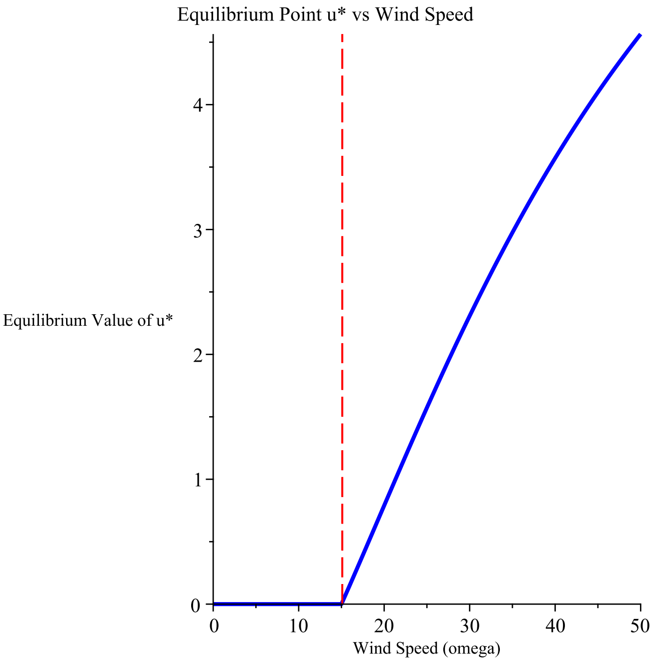

Fig. 1. The bifurcation diagram of u^* with respect to ω.

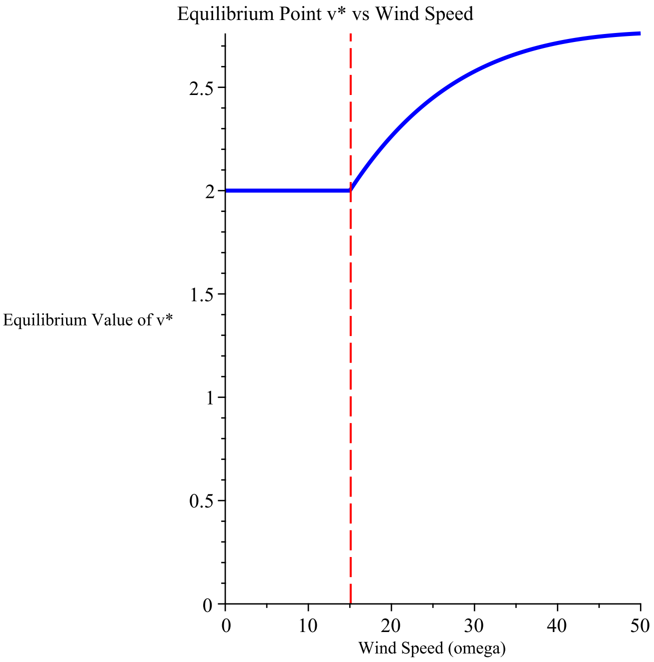

Fig. 2. The bifurcation diagram of v^* with respect to ω.

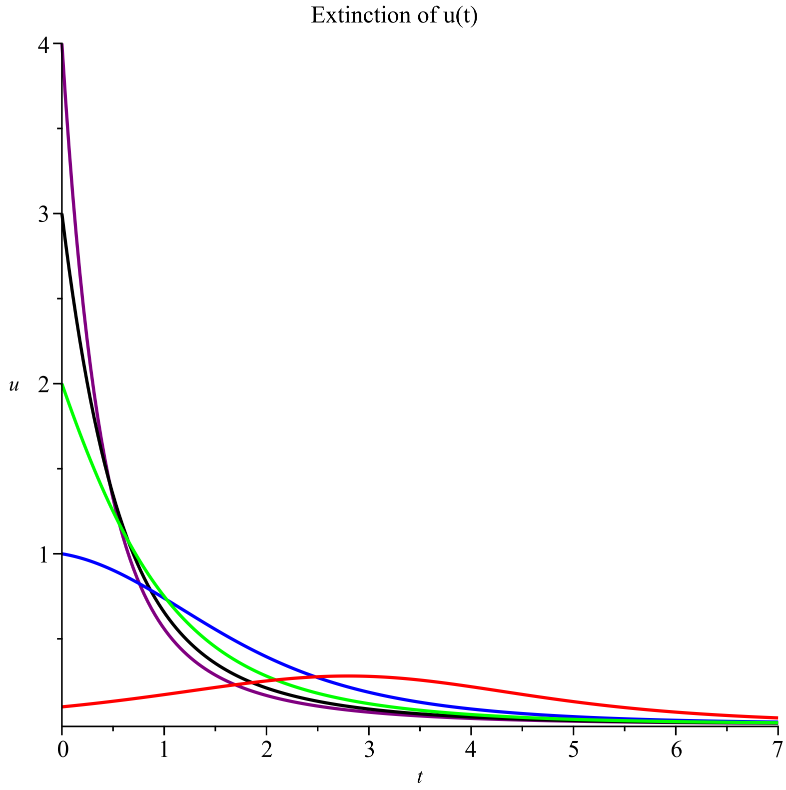

Fig. 3. Time series solution $u(t)$ of the system (56), the initial condition $(u(0), v(0)) = (1, 1)$, $(2, 2)$, $(3, 3)$, $(4, 4)$ and $(0.1, 0.1)$, respectively.

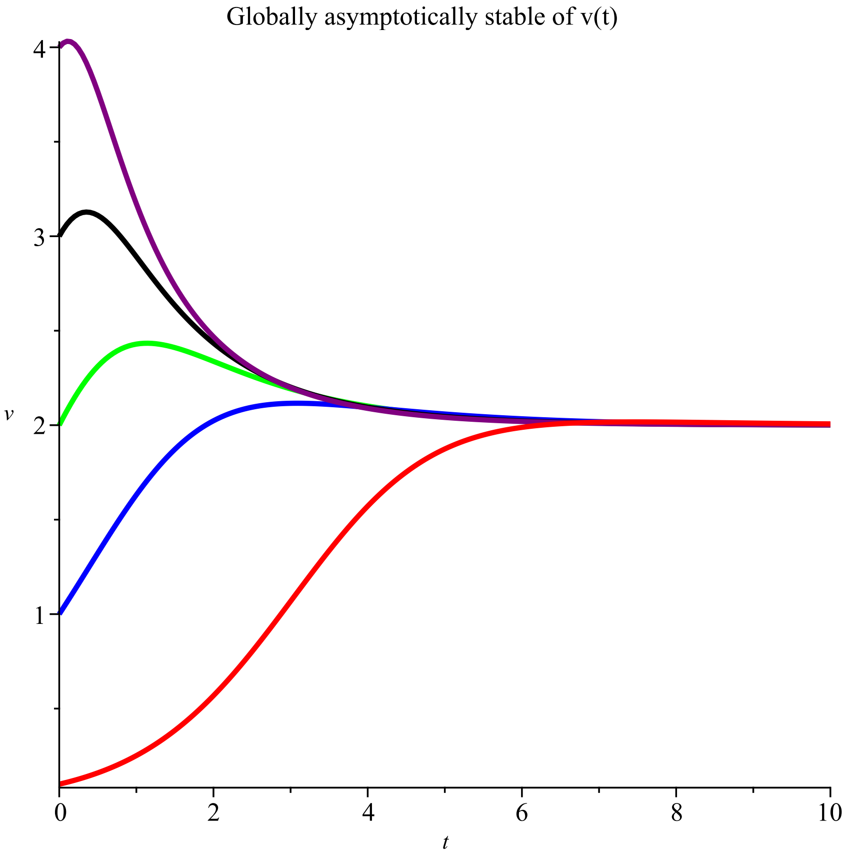

Fig. 4. Time series solution $v(t)$ of the system (56), the initial condition $(u(0), v(0)) = (1, 1)$, $(2, 2)$, $(3, 3)$, $(4, 4)$ and $(0.1, 0.1)$, respectively.

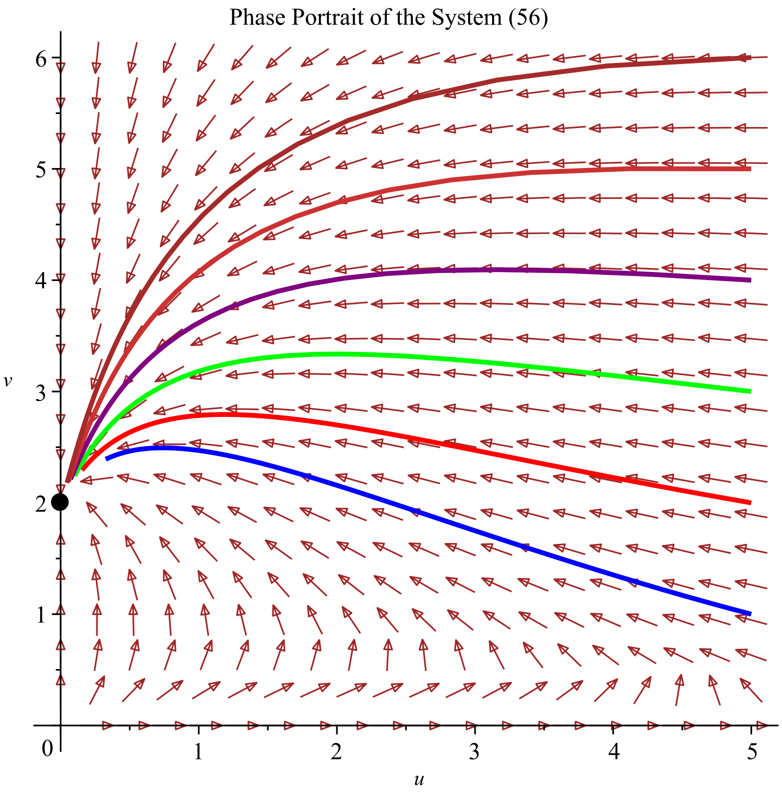

Fig. 5. Phase ortrait of the system (56), the initial condition $(u(0), v(0)) = (8, 1)$, $(8, 2)$, $(8, 3)$, $(8, 4)$ and $(8, 6)$, respectively.

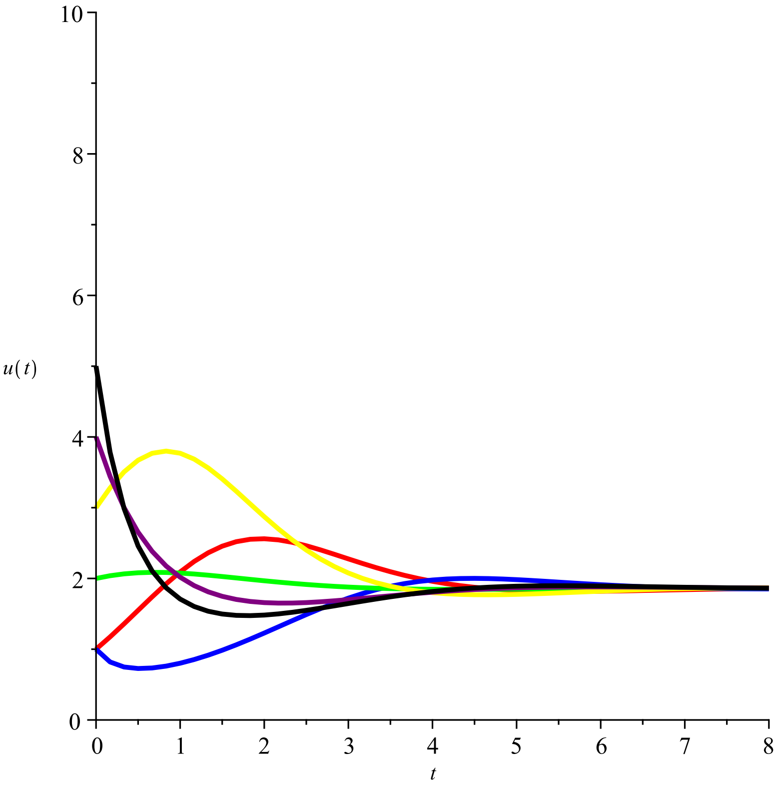

Fig. 6. Time series solution $u(t)$ of the system (58), the initial condition $(u(0), v(0)) = (1, 1)$, $(1, 5)$, $(2, 2)$, $(3, 1)$, $(4, 3)$ and $(5, 4)$, respectively.

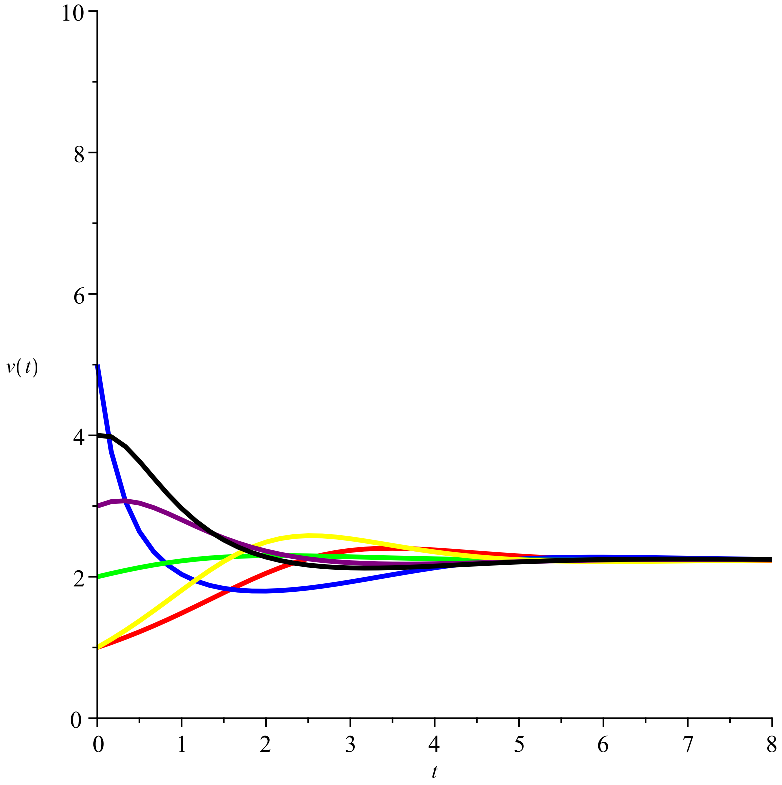

Fig. 7. Time series solution $v(t)$ of the system (58), the initial condition $(u(0), v(0)) = (1,1)$, $(1,5)$, $(2,2)$, $(3,1)$, $(4,3)$ and $(5,4)$, respectively.

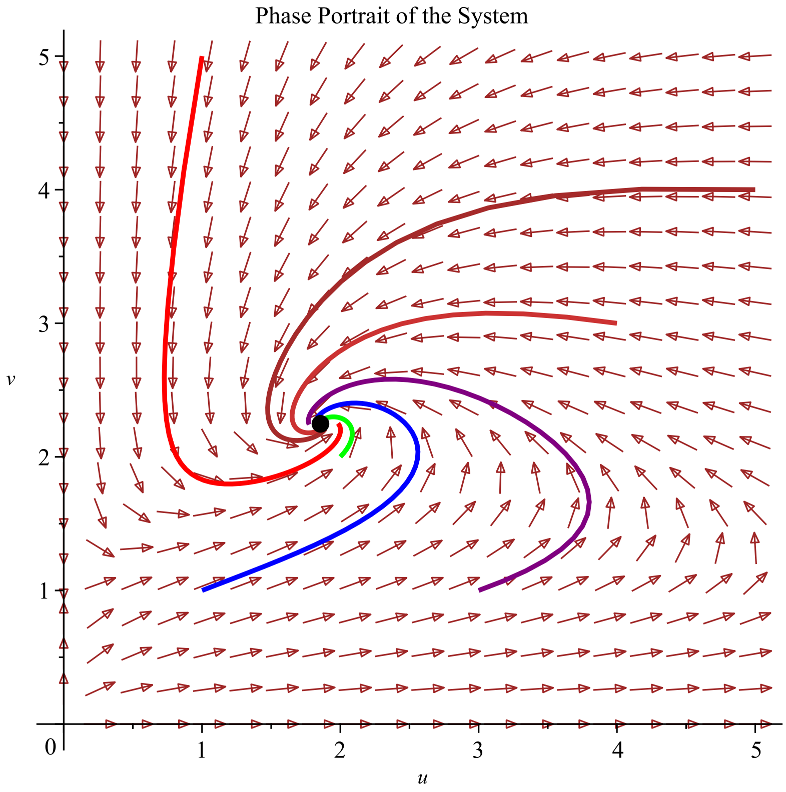

Fig. 8. Phase portrait of the system (58), the initial condition $(u(0), v(0)) = (1,1)$, $(1,5)$, $(2,2)$, $(3,1)$, $(4,3)$ and $(5,4)$, respectively.

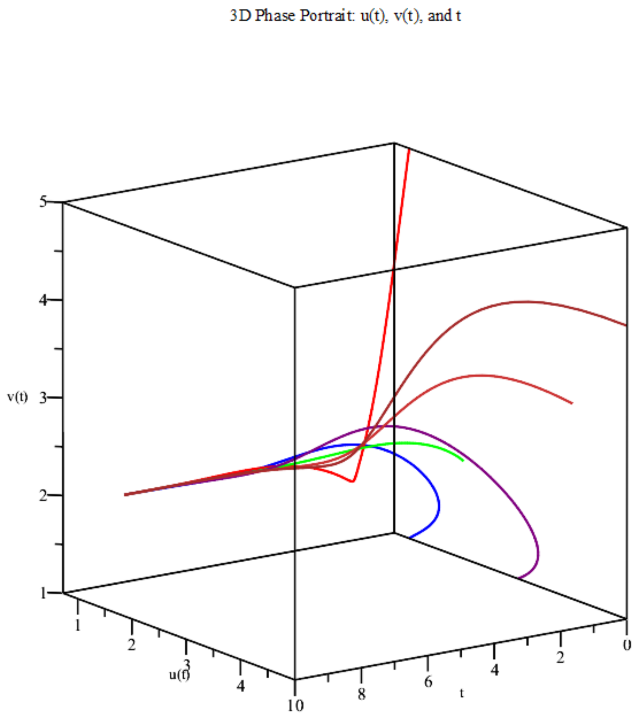

Fig. 9. Phase ortrait of the system (58), the initial condition $(u(0), v(0)) = (1, 1)$, $(1, 5)$, $(2, 2)$, $(3, 1)$, $(4, 3)$ and $(5, 4)$, respectively.

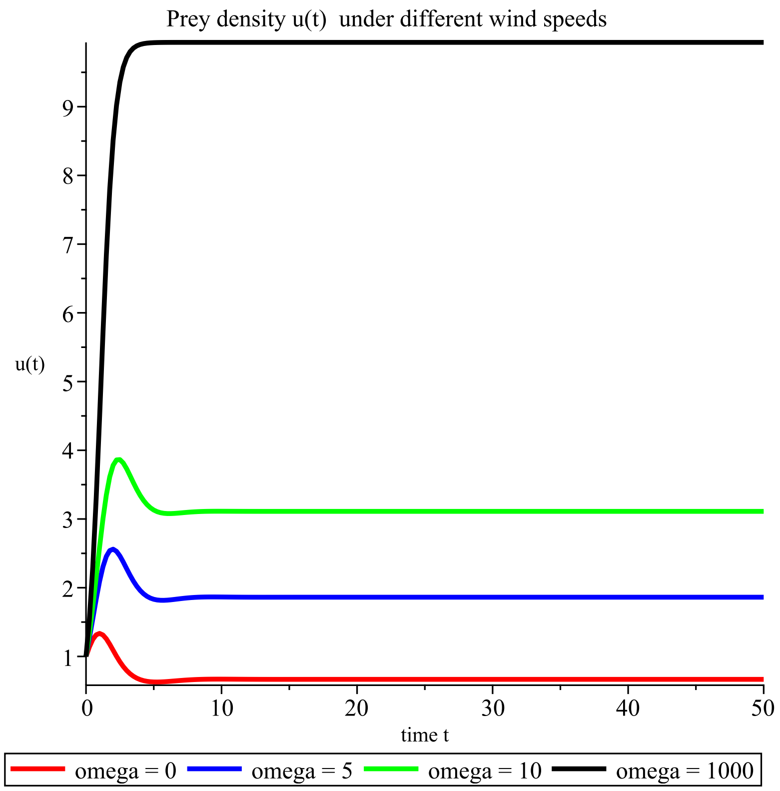

Fig. 10. $u(t)$ corresponding to different values of ω in system (59), the initial condition $(u(0), v(0)) = (1, 1)$, $\omega = 0, 5, 10, 1000$, respectively.

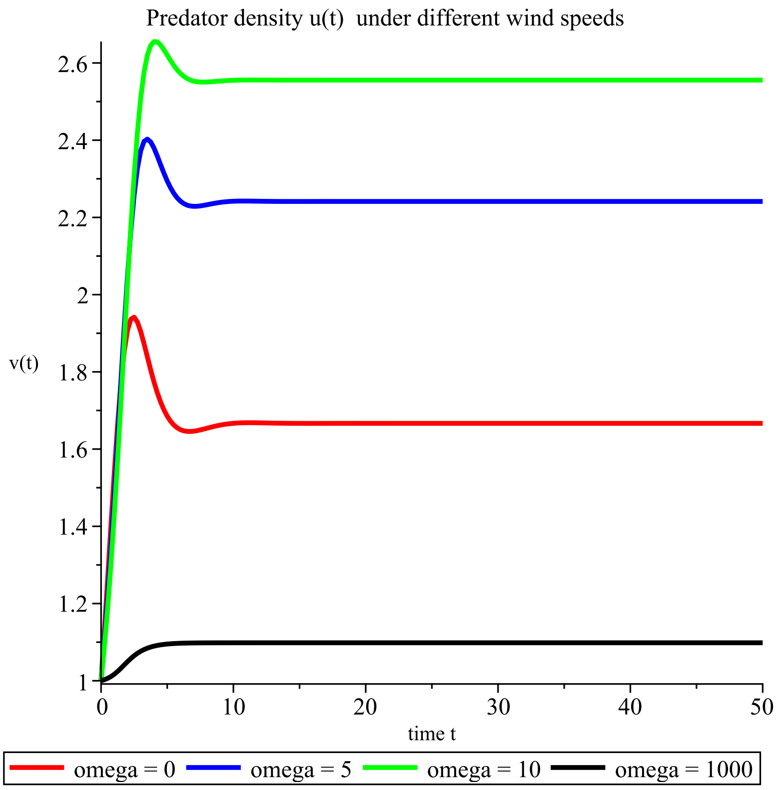

Fig. 11. $v(t)$ corresponding to different values of ω in system (59), the initial condition $(u(0), v(0)) = (1, 1)$, $\omega = 0, 5, 10, 1000$, respectively.

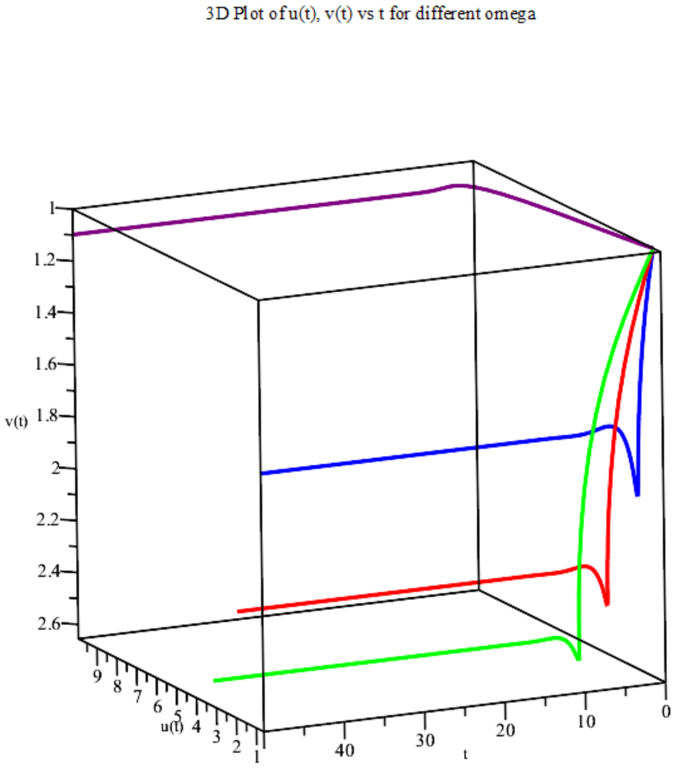

Fig. 12. 3D Plot of $u(t), v(t)$ vs t for different values of ω in system (59), the initial condition $(u(0), v(0)) = (1, 1)$, $\omega = 0, 5, 10, 1000$, respectively.

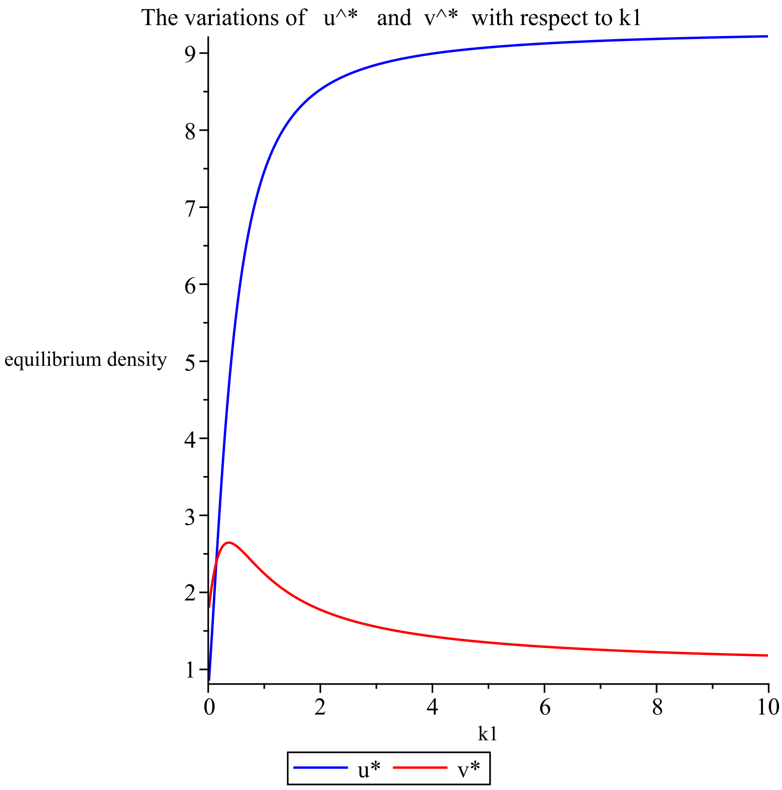

Fig. 13. The variations of u^* and v^* with respect to k_1.

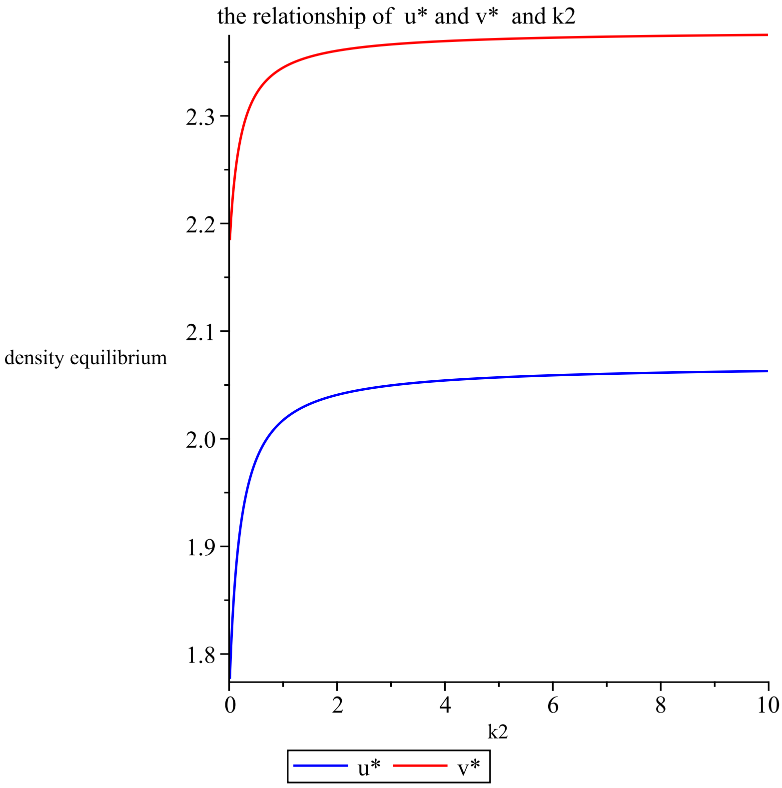

Fig. 14. The variations of u^* and v^* with respect to k_2.

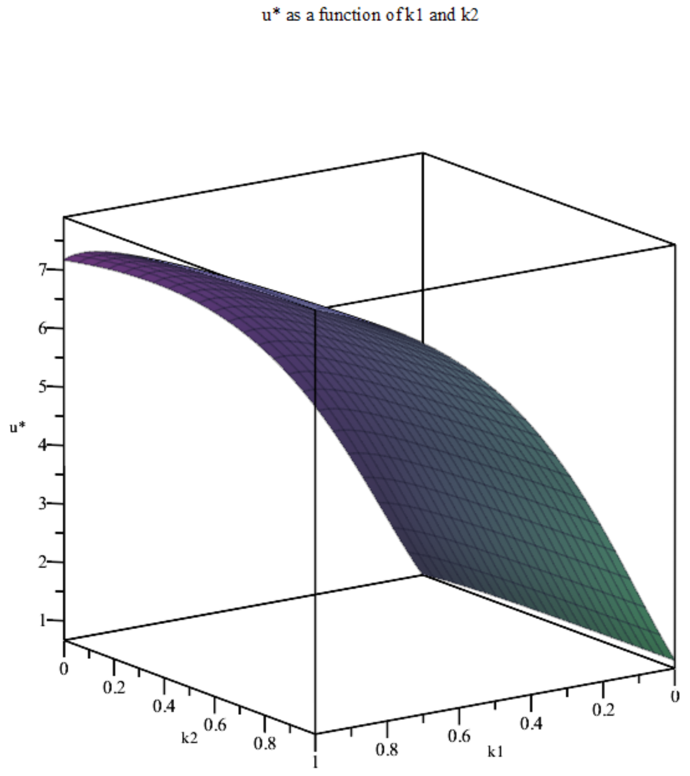

Fig. 15. The variations of u^* with respect to k_1 and k_2.

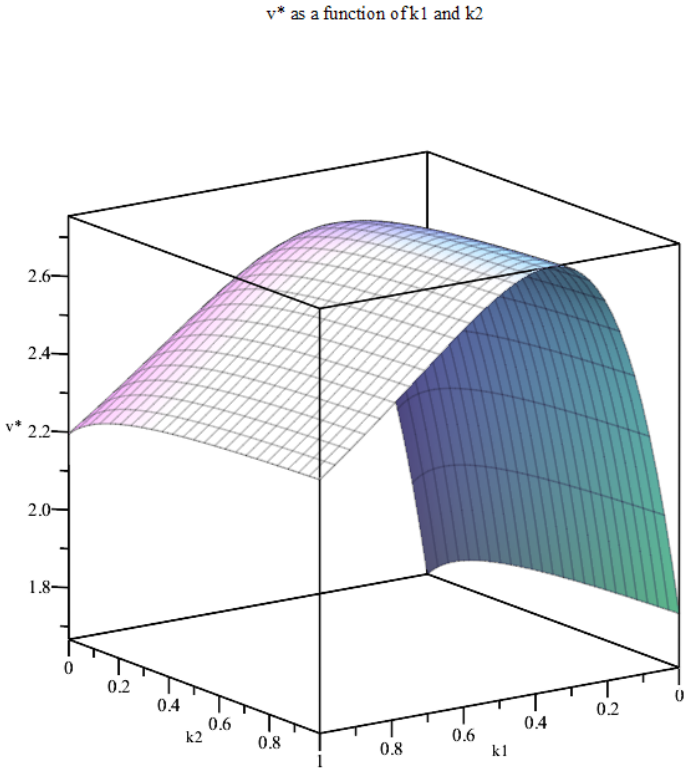

Fig. 16. The variations of v^* with respect to k_1 and k_2.

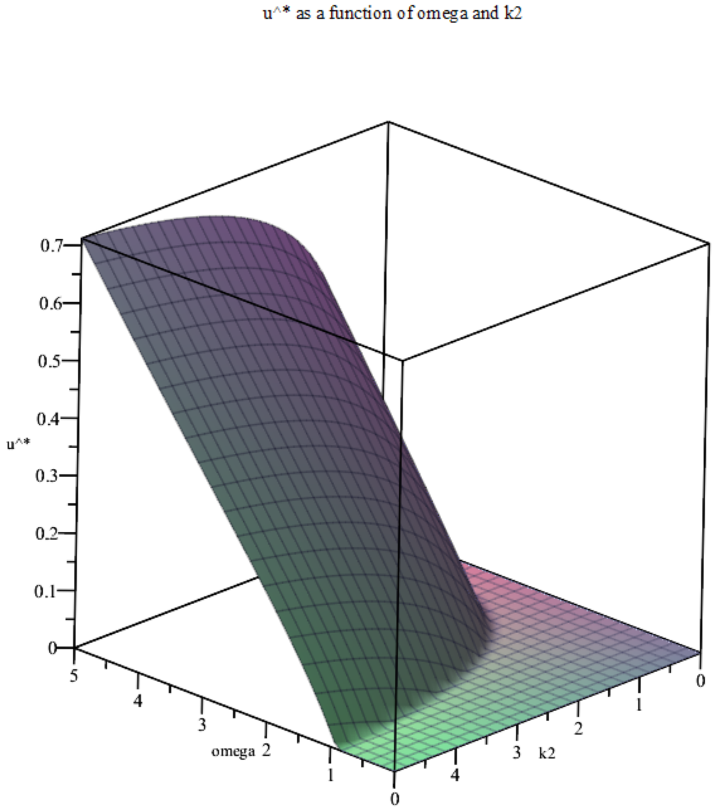

Fig. 17. The variations of u^* with respect to ω and k_2.

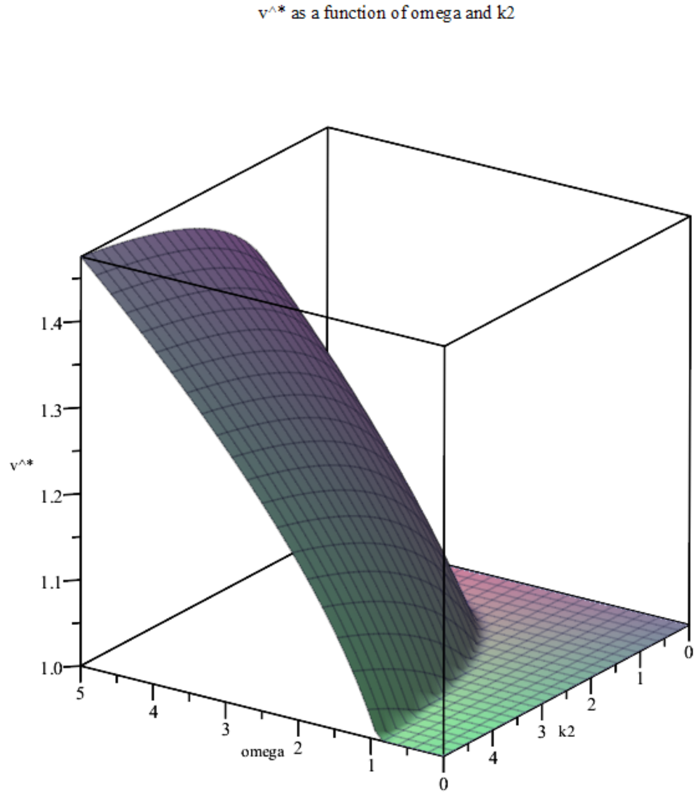

Fig. 18. The variations of v^* with respect to ω and k_2.